A Recirculating Eddy Promotes Subsurface Particle Retention in an Antarctic Biological Hotspot

Katherine L Hudson[1], Matthew John Oliver[1], Josh Kohut[2], Michael S. Dinniman[3], John Klinck[4], Carlos Moffat[1], Hank Statscewich[5], Kim S. Bernard[6], and William Fraser[7]

[1]University of Delaware
[2]Rutgers State University of New Jersey
[3]Old Dominion University
[4]Center for Coastal Physical Oceanography
[5]University of Alaska Fairbanks
[6]Oregon State University
[7]Polar Oceans Research Group

November 24, 2022

Abstract

Palmer Deep Canyon is one of the biological hotspots associated with deep bathymetric features along the Western Antarctic Peninsula. The upwelling of nutrient-rich Upper Circumpolar Deep Water to the surface mixed layer in the submarine canyon has been hypothesized to drive increased phytoplankton biomass productivity, attracting krill, penguins and other top predators to the region. However, observations in Palmer Deep Canyon lack a clear in-situ upwelling signal, lack a physiological response by phytoplankton to Upper Circumpolar Deep Water in laboratory experiments, and surface residence times that are too short for phytoplankton populations to reasonably respond to any locally upwelled nutrients. This suggests that enhanced local upwelling may not be the mechanism that links canyons to increased biological activity. Previous observations of isopycnal doming within the canyon suggested that a subsurface recirculating feature may be present. Here, using in-situ measurements and a circulation model, we demonstrate that the presence of a recirculating eddy may contribute to maintaining the biological hotspot by increasing the residence time at depth and retaining a distinct layer of biological particles. Neutrally buoyant particle simulations showed that residence times increase to upwards of 175 days with depth within the canyon during the austral summer. In-situ particle scattering, flow cytometry, and water samples from within the subsurface eddy suggest that retained particles are detrital in nature. Our results suggest that these seasonal, retentive features of Palmer Deep Canyon are important to the establishment of the biological hotspot.

A Recirculating Eddy Promotes Subsurface Particle Retention in an Antarctic Biological Hotspot

K. Hudson[1], M.J. Oliver[1], J. Kohut[2], M.S. Dinniman[3], J. Klinck[3], C. Moffat[1], H. Statscewich[4], K. Bernard[5], and W. Fraser[6]

[1]College of Earth, Ocean, and Environment, University of Delaware, Lewes, Delaware, USA; [2]Department of Marine and Coastal Sciences, Rutgers, The State University of New Jersey, New Brunswick, New Jersey, USA; [3]Department of Ocean and Earth Sciences, Old Dominion University, Norfolk, VA, USA; [4]College of Fisheries and Ocean Sciences, University of Alaska, Fairbanks, Fairbanks, Alaska, USA; [5]College of Earth, Ocean, and Atmospheric Sciences, Oregon State University, Corvallis, Oregon, USA; [6]Polar Oceans Research Group, Sheridan, Montana, USA.

Corresponding author: K. Hudson (khudson@udel.edu)

Key Points:

- Isopycnal doming over Palmer Deep Canyon suggests the presence of a closed, subsurface, cyclonic eddy over the canyon
- Subsurface eddy increases retention time of simulated particles at depth
- A persistent, subsurface particle layer, retained by the eddy, consists of individual detritus particles on the order of 70 microns

Abstract

Palmer Deep Canyon is one of the biological hotspots associated with deep bathymetric features along the Western Antarctic Peninsula. The upwelling of nutrient-rich Upper Circumpolar Deep Water to the surface mixed layer in the submarine canyon has been hypothesized to drive increased phytoplankton biomass productivity, attracting krill, penguins and other top predators to the region. However, observations in Palmer Deep Canyon lack a clear in-situ upwelling signal, lack a physiological response by phytoplankton to Upper Circumpolar Deep Water in laboratory experiments, and surface residence times that are too short for phytoplankton populations to reasonably respond to any locally upwelled nutrients. This suggests that enhanced local upwelling may not be the mechanism that links canyons to increased biological activity. Previous observations of isopycnal doming within the canyon suggested that a subsurface recirculating feature may be present. Here, using in-situ measurements and a circulation model, we demonstrate that the presence of a recirculating eddy may contribute to maintaining the biological hotspot by increasing the residence time at depth and retaining a distinct layer of biological particles. Neutrally buoyant particle simulations showed that residence times increase to upwards of 175 days with depth within the canyon during the austral summer. In-situ particle scattering, flow cytometry, and water samples from within the subsurface eddy suggest that retained particles are detrital in nature. Our results suggest that these seasonal, retentive features of Palmer Deep Canyon are important to the establishment of the biological hotspot.

Plain Language Summary

Palmer Deep Canyon is an area of high biological activity along the Western Antarctic Peninsula. These biological hotspots were once thought to be driven by the upwelling of deep, nutrient-rich water promoting phytoplankton growth. Previous observations illustrated a lack of upwelling within Palmer Deep Canyon and suggested that a subsurface feature may instead drive the increased biological activity in the region. We found that a subsurface, closed eddy increases residence times of deep particles over Palmer Deep Canyon. This feature can retain particles through the productive summer months and may be important to the establishment of the biological hotspot.

1.0 Introduction

Palmer Deep Canyon (PDC) is the nearshore deep terminus of a cross-shelf canyon along the West Antarctic Peninsula (WAP; Figure 1). Like many similar canyons along the WAP, PDC is a known biological hotspot due to its association with high predator activity, penguins in particular (Carvalho et al., 2016, 2020; W. R. Fraser & Trivelpiece, 1996; Schofield et al., 2013). Some colonies of Adélie penguins in this region of the WAP have persisted on millennial timescales (S. Emslie et al., 1998; S. D. Emslie & Patterson, 2007), indicating that this location is a persistent focal point of upper trophic level activity. The spatial coherence of penguin foraging regions and submarine canyons along the WAP led to the 'canyon hypothesis' by Fraser & Trivelpiece (1996) that suggests that the physical oceanography in the region that results from the presence of PDC and other canyons along the WAP drive the formation of the biological hotspots (W. R. Fraser & Trivelpiece, 1996; Schofield et al., 2013). Since the hypothesis was coined, polar researchers have searched for the driving mechanisms responsible for connecting canyons with increased biological activity.

Prézelin et al. (2000; 2004) suggested that upwelling of deep, nutrient-rich Upper Circumpolar Deep Water (UCDW) on the continental shelf may promote phytoplankton blooms over the shelf, which could provide a sufficient food source for krill, a local keystone species and an important prey source for local penguin colonies. These upwelling regions, Prézelin et al. (2000) argued, were within the foraging range (100-150 km) for Adélie penguin populations based near PDC (W. R. Fraser & Trivelpiece, 1996). However, satellite telemetry of Adélie penguins nesting near PDC later revealed that these penguins forage within 20 km of their colonies, and specifically over PDC (Oliver et al., 2013, 2019; Pickett et al., 2018). This suggested that more localized physical processes may be responsible for the formation of the biological hotspot within PDC. With wind strength helping move UCDW onto the shelf, cross-shelf canyons can act as conduits for UCDW transport onto the continental shelf (Dinniman et al., 2012; Martinson & McKee, 2012; Moffat et al., 2009). Autonomous gliders deployed within PDC observed the shoaling of warm, subsurface waters over the canyon nearshore terminus (Schofield et al., 2013). They suggested this water mass was a modified derivative of UCDW (mUCDW), which can be transported onshore via subsurface eddies and canyons along the continental shelf (Couto et al., 2017; Schofield et al., 2013). In addition, a multi-year analysis of satellite-derived sea ice concentration, sea surface temperature, and chlorophyll suggested that

sea ice concentration was lower, sea surface temperature was higher, and chlorophyll was higher over PDC in comparison to nearby (~10 km) shelf areas (Kavanaugh et al., 2015). Together, these results suggested that mUCDW was upwelling within the canyon, providing the warmth to melt surface sea ice and the nutrients to fuel phytoplankton blooms, which would in turn feed krill and their predators (Kavanaugh et al., 2015).

However, extended seasonal *in-situ* observations within PDC have suggested that local, seasonal upwelling of mUCDW may be rare in the austral summer in PDC. Analysis of temperature and salinity properties from an extensive glider data set within PDC suggests that Winter Water (WW) acts as a barrier between the upward ventilation of mUCDW and the surface mixed layer in the austral summer (Carvalho et al., 2016; Hudson et al., 2019). Carvalho et al. (2020) tested the hypothesis that the upwelling of mUCDW could enhance phytoplankton growth experimentally by exposing surface phytoplankton communities to mUCDW waters. There were no significant changes in phytoplankton physiology when communities were exposed to nutrient-rich mUCDW (Carvalho et al., 2020). Furthermore, Kohut et al. (2018) calculated surface residence times within the penguin foraging grounds over PDC based on surface current measurements from a High-Frequency Radar system and estimated surface residence times on the order of ~2 days. Since the estimated local doubling time for phytoplankton is on the order of ~7-70 days (Moline, 1998), they argued that the observations of increased phytoplankton concentrations over the canyon could not be due to local episodic upwelling events because the surface residence time was too short to for phytoplankton to respond to upwelled nutrients (Kohut et al., 2018).

Time series of the water mass properties suggest isopycnal doming is present, which led to the hypothesis that a subsurface recirculating eddy may be present within PDC (Hudson et al., 2019). Gliders deployed within PDC also observed a subsurface backscattering layer over the deepest portions of PDC (Hudson et al., 2019). Hudson et al. (2019) hypothesized that this layer was made up of mostly aggregations of marine snow and other biogenic particles, possibly exported from the surface layer. The persistence of this particle layer suggested that it could be a result of higher residence times due to recirculation, thus retained within the eddy and over PDC (Hudson et al., 2019).

Here, we test the hypotheses that a persistent subsurface eddy exists in the PDC and is the likely explanation for the associated subsurface particle layer proposed by Hudson et al. (2019)

using simulations from the WAP conducted with the Regional Ocean Modeling System (ROMS) domain. We verify these simulations with glider deployments and surface measurements from a High-Frequency Radar (HFR) system deployed in 2015 and 2020. First, we examine model density properties and currents to show that a subsurface eddy exists within PDC. Second, we use neutrally buoyant particle simulations in ROMS to calculate the residence of particles within the eddy. We hypothesize that neutrally buoyant particles will have longer residence times over the PDC compared to nearby regions. Third, we use glider-measured optical backscatter, and an Imaging Flow CytoBot (IFCB) to describe the subsurface particle layer first observed by Hudson et al. (2019) that is potentially being retained within the canyon. We hypothesize that these particles are aggregates of marine snow that originate from the surface. If there is a subsurface eddy present within PDC, it could potentially act as a retaining feature for detrital particles that could be a food resource for other zooplankton.

2.0 Methods

2.1 Regional Ocean Modeling System

2.1.1 Model Simulations

ROMS (Haidvogel et al. 2008) was used to test the hypothesis that a subsurface eddy exists within PDC. The implementation of ROMS for the WAP (Graham et al., 2016) has 1.5 km horizontal resolution and 24 vertical layers and includes a dynamic ice model (Budgell, 2005) and the interactions between floating ice shelves and the ocean underneath (Dinniman et al., 2011; Holland & Jenkins, 1999). Atmospheric forcing is from archived forecasts from the Antarctic Mesoscale Prediction System (Powers et al., 2012). The model used here has two important updates from the version described in Graham, Dinniman, and Klinck (2016). The base bathymetry (Bedmap2; Fretwell et al. 2013) was updated around Anvers Island (including PDC and the southern Gerlache Strait) using GMRTv3.6 (Global Multi-Resolution Topography; Ryan et al., 2009) multibeam data. Also, tidal forcing was added at the model lateral boundaries using tidal sea surface height and velocity from the CATS2008 regional Antarctic tidal model (Padman et al., 2002).

The model was run from November 2008 to April 2009. Since the model simulations were conducted for a different year than the glider observations, ROMS and glider data were

both averaged over the same seasonal time (early January to early March; see Section 2.2). The subsurface eddy is hypothesized to be a seasonal feature; therefore, we believe that this seasonal averaging will overcome the time misalignment between the model and *in-situ* data. Average temperature, salinity, and potential density (σ_θ) were calculated for each of the three transects (along-canyon, deep across-canyon, and shelf-canyon) (Figure 1b). The averaged cross-sections had the same horizontal resolution as the model (1.5 km). The vertical resolution was variable since ROMS 24 sigma coordinate depth layers are terrain following. These layers were used to create the cross-sections and translated to a 1 m vertical grid for plotting. Current velocities and sea surface height (SSH) anomalies from the model were averaged in each model grid cell over the study region (Figure 1b). Mixed Layer Depth (MLD) was estimated in each grid cell and averaged over PDC for each day using the max Brunt-Vaisala frequency (N^2; Carvalho et al., 2017).

2.1.2 Particle Simulations & Residence Time Calculations

Neutrally-buoyant particles were released in the model simulation on a grid with approximately 4 km horizontal spacing around PDC (Figure 1a). The particles were advected within the model code at every model time step (50 sec) using the full three dimensional velocity fields of the model (at the time and position of each particle) plus a random walk in the vertical direction which is a function of the parameterized model vertical diffusion (Hunter et al., 1993; Visser, 1997). Particle positions were saved hourly. The vertical random walk was included for all particle releases, except for surface releases. Particles were released every 2 days starting on November 1, 2008 until the end of March 2009. All particle releases were tracked for a minimum of 30 days and a total of 64,800 particles were released. Particles were released at the surface, 10, 20, 50, 120, 150, and 300 m.

Residence times were calculated using e-folding time which is the time to needed for the concentration of particles to drop to 1/e (~37%) within a defined region (Couto et al., 2017; Kohut et al., 2018; Piñones et al., 2011). Residence times were calculated in three regions within the model domain: PDC, the continental shelf, and the coast of Anvers Island (Figure 1a). The 400 m isobath from ROMS was used to define PDC, similar to Couto et al. (2017). The residence time was calculated for each particle release event from December 2008 to February 2009 to focus on the height of the austral summer when predator foraging activity within PDC is highest

(Smith et al., 1995). Residence times were compared statistically in R with a Kruskal-Wallis test and Dunn post-hoc test with Bonferroni correction for multiple tests (R Core Team, 2020).

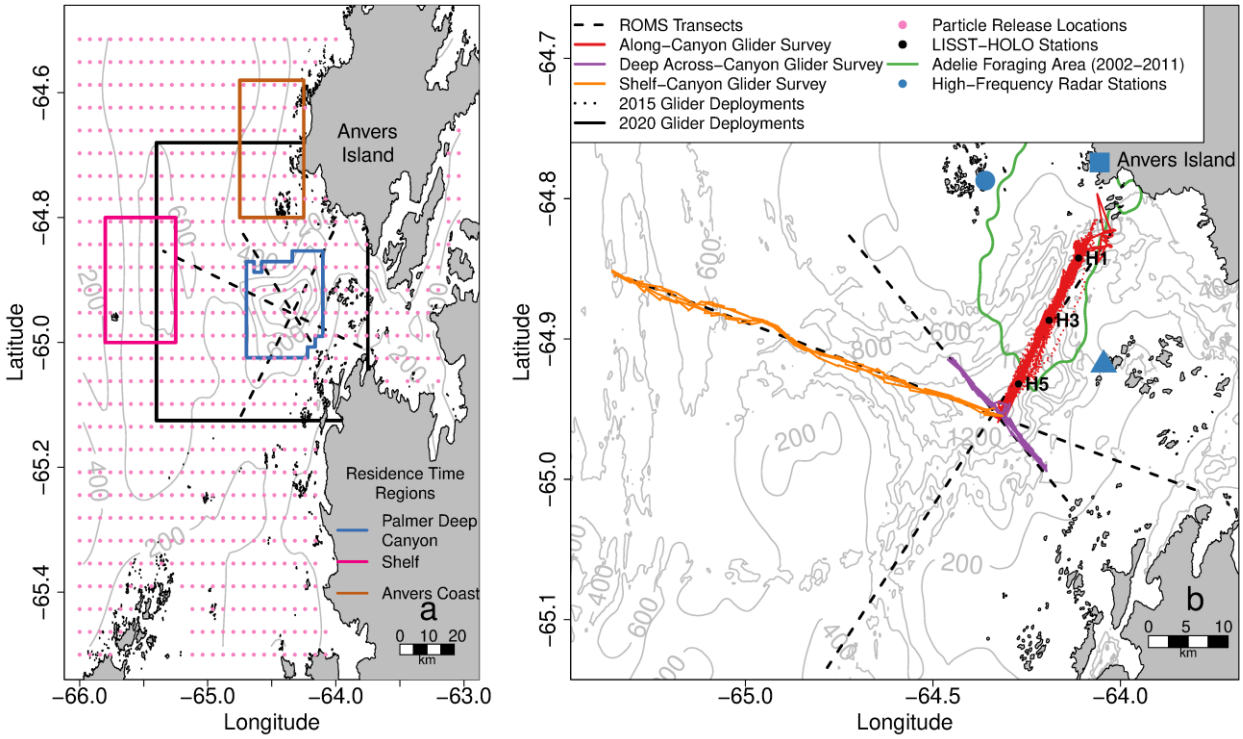

Figure 1. (a) Bathymetric map of Palmer Deep Canyon (PDC) and the surrounding shelf area. Bathymetry is ROMS bathymetry. Pink points illustrate where neutrally buoyant particles were seeded in ROMS experiments. The black box outlines the area shown in panel b. The colored boxes indicate regions used for residence time calculations. (b) Bathymetric map of PDC and the glider transects from both field campaigns used in this analysis, with bathymetry from GMRT (Ryan et al., 2009). The black dashed lines in both panels indicate the corresponding transects used in ROMS. The green line represents the 99.5% contour for Adélie penguin foraging locations for penguins tagged between 2002 and 2011. The black circles indicate the locations of LISST-HOLO stations sampled in 2020. The blue shapes represent high-frequency radar locations at Palmer Station (square), Joubin Islands (circle), and Wauwerman Islands (triangle).

2.2 Glider Data Collection

The glider data used in this analysis was collected over the 2014-2015 and 2019-2020 austral summers. The 2015 glider deployments are described in Hudson et al. (2019). Only temperature, salinity, σ_θ, and optical backscatter variables are used in this analysis.

In the austral summer of 2020, three Slocum electric gliders were deployed. Two of the three gliders were deployed on 9 January 2020 and the third glider was deployed on 11 January 2020. One of the gliders was recovered on 26 February and the remaining two gliders were recovered by 11 March 2020. For this analysis, we focus on the following transects covered by

the gliders: the along-canyon transect, from the head of the canyon to the deepest portion of the canyon; the deep across-canyon transect, which ran perpendicular to the along-canyon transect over the deepest portion of PDC; and the shelf-canyon transect, which traveled from the deepest portion of the canyon, over the canyon sill (Figure 1b). The same along-canyon transect was sampled in both 2015 and 2020. The deep across-canyon and shelf-canyon lines were sampled opportunistically in 2020. The deep across-canyon transect was sampled a total of four times between 14 January and 3 March 2020. The shelf-canyon transect was sampled twice between 22 January and 11 February 2020. In 2020, a total of 1214 profiles were completed on the along-canyon transect. On the deep across-canyon transect, 139 profiles were completed, and 197 profiles were completed on the shelf-canyon transect. In 2015, the along-canyon transect was sampled to 200 m depth, while in 2020, this transect was sampled to 1000 m depth. Both the shelf-canyon and deep across-canyon transect were sampled to 1000 m depth.

Each glider was equipped with a pumped Seabird conductivity, temperature, and depth (CTD) sensor and a WetLabs Ecopuck, which measured optical backscatter at 700 nm and chlorophyll concentration using fluorescence. All gliders also measured oxygen saturation, either with an Aanderaa or RinkoII optode. The Seabird CTDs were factory calibrated in August 2014, January 2019, and April 2019. Optical data from the gliders were cross-calibrated using data from when the gliders were in close proximity with each other (supporting information Text S1, Equations S1-4, Figure S1), similar to how the gliders were cross-calibrated in 2015 (Hudson et al. 2019). These corrections were applied to the 2020 glider data set. Temperature and salinity properties were used to calculate density and σ_θ, which was calculated using the *swSigma0* function in R package *oce* (Kelley & Richards, 2020; R Core Team, 2020). Optical data were only collected on upcasts. The bathymetry data from GMRTv3.6 (Ryan et al., 2009) was matched to 2015 and 2020 glider data.

Average cross sections were generated from the glider data by averaging in-situ measurements in 2 km horizontal bins and 5 m vertical bins. This was done separately for each field campaign. Stratification strength was estimated using N^2, calculated using the *swN2* function in *oce* (Kelley & Richards, 2020; R Core Team, 2020). The max N^2 was calculated each individual glider profile performed on the along-canyon transect in 2015 and 2020. Only profiles deeper than 50 m were considered following Carvalho et al. (2017). MLD was estimated using maximum N^2 (Carvalho et al., 2017).

2.3. High-Frequency Radar

A High-Frequency Radar (HFR) system was deployed around PDC in 2015 and 2020 (Figure 1b). The 2015 deployment is described in Kohut et al. (2018) and the 2020 deployment of this system was the same for the purposes of data collection. This system measures determines surface currents by analyzing and processing the Doppler spectrum of backscattered radio waves (Barrick et al., 1985; Kohut et al., 2018). These currents are believed to be representative of currents within the mixed layer in PDC and the surrounding region (Carvalho et al., 2017; Kohut et al., 2018). Weather stations were deployed with the HFR stations to measure wind speeds. Using this wind data, we averaged the HFR field in periods where winds were low (< 5 m s^{-1}) at the Joubin and Wauwerman Islands (on opposite sides of the canyon; Figure 1b) for at least 12 hours.

2.4 Imaging Flow CytoBot

An Imaging Flow CytoBot (IFCB) was utilized in two sampling events to characterize the subsurface particle layer. The first sampling event occurred on 8 February 2020, and the second occurred on 7 March 2020. For both sampling events, stations HOLO 5, 3, and 1 were sampled (Figure 1b). A Rosette equipped with a Seabird SBE-19 Plus V2 CTD (factory calibrated July 2019) and 6 Niskin bottles was deployed to 200 m. Bottles fired at 5, 35, 75, 100, 150, and 200 m on the upcast for both sampling events. Water from each depth was collected in dark 50 ml Falcon tubes. The Falcon tubes were triple rinsed with sample water before the sample was collected. Tubes were kept in the dark until they were brought back to the lab, where they were kept dark and cold until processed.

Images were collected with both the scattering (PMTA) and chlorophyll (PMTB) sensors on. Sensitivities were increased to allow for maximum photo collection without producing high numbers of photos with no targets, following the Palmer Long Term Ecological Research (LTER) program protocol. Blob and feature extraction were performed using the MATLAB IFCB Toolbox developed by Dr. Heidi Sosik (Olson & Sosik, 2007; https://github.com/hsosik/ifcb-analysis/wiki). Data were matched to CTD profiles after analysis.

To estimate numbers of live versus detrital cells imaged by the IFCB, we used PMTB to classify cells as either live cells or detritus. Any images with PMTB greater than 0.01 (~77% quantile) were classified as live cells. This threshold was based on the distribution of PMTB

values and glider-observed chlorophyll concentrations. Equivalent diameter, as estimated by the IFCB Toolbox, was used to estimate particle size.

3.0 Results

3.1 Subsurface Eddy

3.1.1 ROMS Simulations

Average velocity vectors over PDC from early January to mid-March show a relatively strong (~10 cm s^{-1}), cyclonic circulation over the canyon (Figure 2; Supplemental Movie 1). This circulation pattern is present across several depths (0, 50, 100, 150, and 300 m) (Figure 2a-e). At shallower depths (0 and 50 m), the mean cyclonic circulation expands beyond the bounds of the canyon (Figure 2a-b). Daily averages show a great deal of variability and many periods where there is not a closed circulation over the canyon (Supplemental Movie 1). As depth increases, the circulation associated with the eddy becomes more closely aligned with isobaths and its horizontal extent more limited with respect to the surface flow (Figure 2c-e). It appears to form in late December and is no longer a coherent feature after late February/early March (Supplemental Movie 1). Consistent with the flow of the eddy being approximately in geostrophic balance, the timing of when the rotation appears is similar the following summer (not shown) but not exactly the same. Mean sea surface height (SSH) over the same time period shows a depression of SSH over the canyon (colored portions of Figure 2). SSH anomaly was approximately -9 cm over PDC during the austral summer and mean flow at all depths was

cyclonic around this low-pressure system (Figure 2).

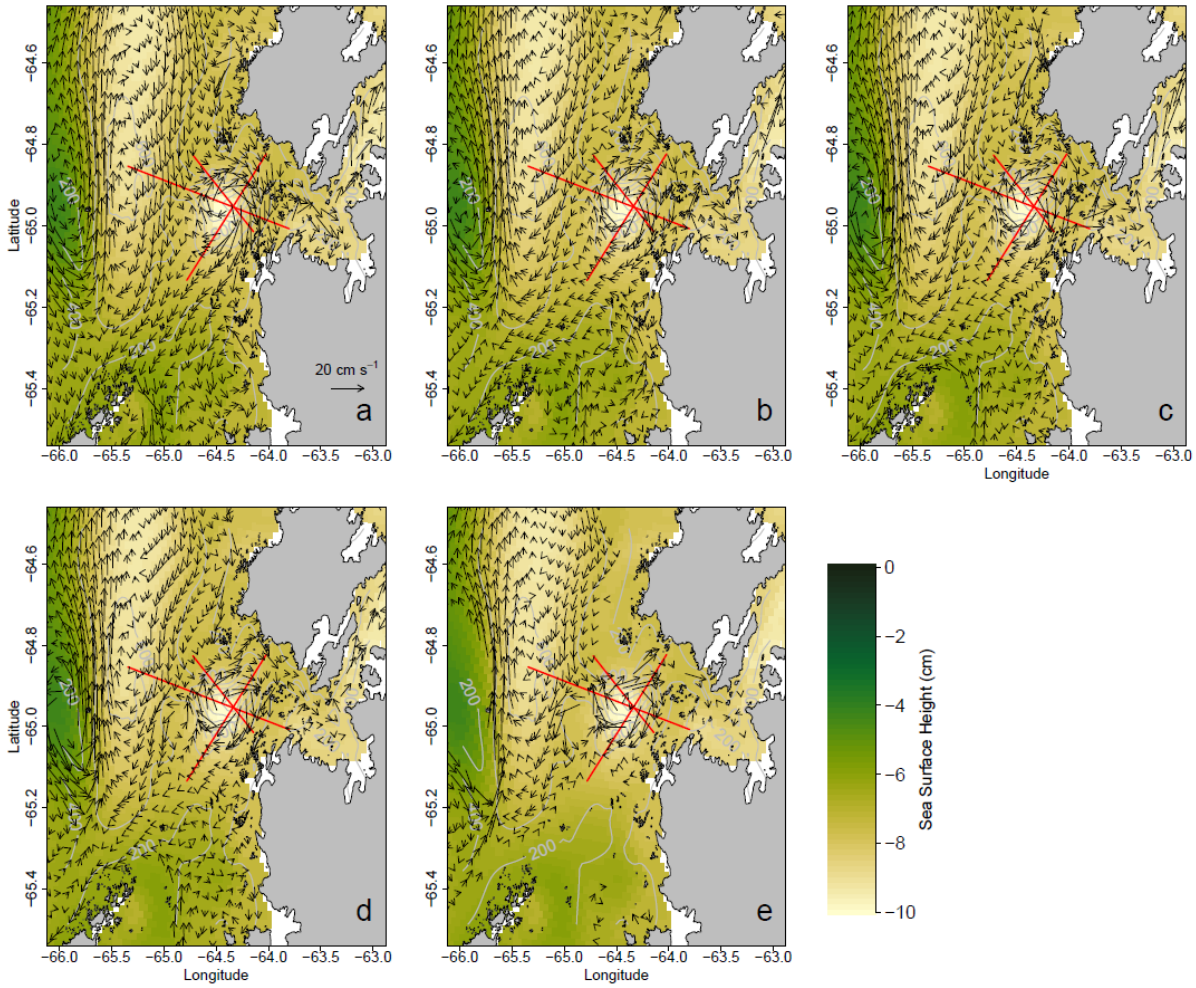

Figure 2. Average current velocity at surface (a), 50 (b), 100 (c), 150 (d), and 300 m (e) in cm s^{-1} over ROMS model domain used in this study from January to March 2009. Color indicates the mean sea surface height (cm) from ROMS over the same time period. Red lines indicate the location of ROMS average transects. Every eighth model vector is plotted.

Isopycnals from ROMS simulation on the along-canyon (Figure 3a) and shelf-canyon (Figure 3b) transects begin to rise over the canyon between approximately 100 and 200 m depth. In both transects, the isopycnals gradually shallow on the southern and western flanks, respectively, of the canyon (Figure 3a-b). Over the sill separating the canyon from the rest of the continental shelf, isopycnals are spaced more evenly in the top 400 m than in comparison to the same isopycnals over PDC, possibly indicative of isopycnal stretching over the canyon (Figure 3b). On the deep-across canyon transect, the model suggests a slight depression of isopycnals beginning just above 100 m, approximately 10 km into the transect, over the deepest portions of the canyon (Figure 3c). There is also a slight lift in isopycnals on the west flank of the canyon,

approximately 20 km along the transect, however, the isopyncals were relatively flat over this transect (Figure 3c).

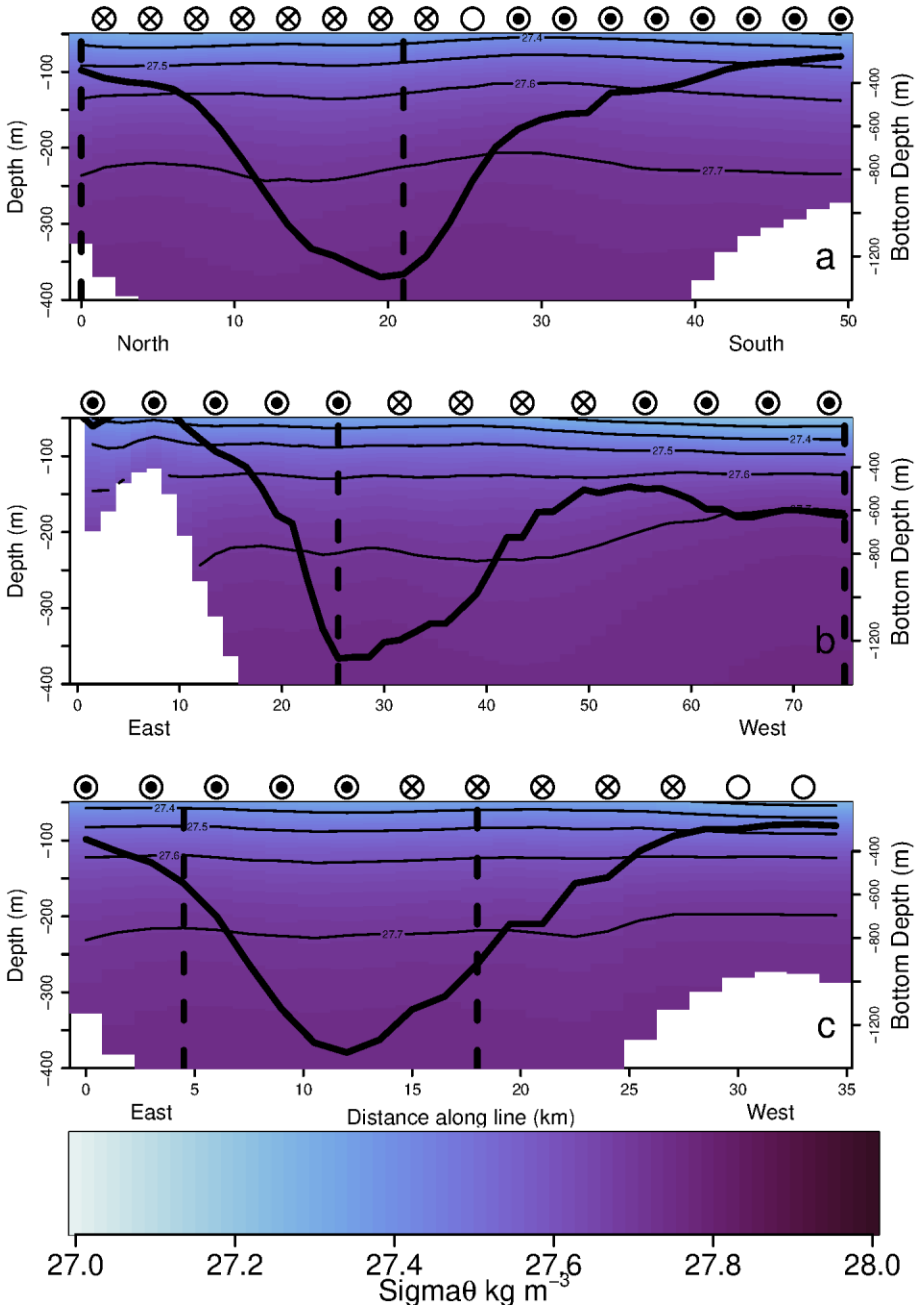

Figure 3. Average σ_θ cross sections with contour lines from the along-canyon (a), shelf-canyon (b), and deep across-canyon (c) transects in ROMS simulation. The start of the transects (0 km) indicates the northern (a) and eastern (b-c) sides of the transects. Observations were averaged in 1.5 km bins in the horizontal. In the vertical, data were averaged over the model's 24 vertical depth bins and translated to 1m depth bins for plotting. Points above each plot indicate general flow into (circles containing an 'x') or out of (circles containing a point) the cross section as illustrated in Figure 2. Empty circles indicate flow parallel to the transect. The black line denotes the model bathymetry and corresponds to the right y axis in each panel. Note that each panel starts at 50m. Vertical dashed black lines indicate the regions of the transects that were occupied by the gliders.

3.1.2 Glider Observations

The gliders in both field campaigns observed similar density structures as in ROMS simulations (Figures 3-4, S4). In 2015, stratification decreased on the along-canyon transect over the course of the glider deployment (Figure S5a) while stratification increased over time in 2020 (Figure S5b). On average, waters were fresher and warmer in the surface in 2020 (Figures S6-S9), resulting in some isopycnals being deeper in the water column than they were in 2015 (Figure 4). On average, both field campaigns reveal surface waters are lighter and deep waters are heavier than ROMS simulations (Figures 3-4), mostly due to differences in the salinity (Figures S2, S3, S7, S9).

The along-canyon transects observed similar uplift of isopycnals over the deepest portions of the canyon in both deployment years (Figure 4a-b). Isopycnals began slowly rising in the water column near the edge of the canyon (~10 km into the transect) (Figure 4a-b). This uplilft was most pronounced between 50 and 100 m in 2015 and between 50 and 150 m in 2020 (Figure 4a-b). The uplift was present, but more gradual below these depths (Figure 4a-b).

The uplift of isopycnals over the canyon is also observed on the shelf-canyon line (Figure 4c). As on the along-canyon line, this uplift is the most prominent in the top 150 m (Figure 4b-c). Like ROMS simulations, the isopycnals also appear to stretch as they move from the continental shelf into the canyon, while this is more pronounced in ROMS (Figures 3b, 4c). On the deep across-canyon line, the isopycnals appear to gradually deepen on the western flank of the canyon (Figure 4d). There is no small dip in isopycnal depth in the glider observations like there was in model simulations (Figures 3c, 4d).

Oxygen saturation reached a minimum of 50% over the deepest portions of the canyon in 2020 (Figure S10). Low oxygen saturation (< 70%) was generally observed higher in the water column over these areas over the deepest portions of PDC, especially on the along-canyon and shelf-canyon transects (Figure S10a-b).

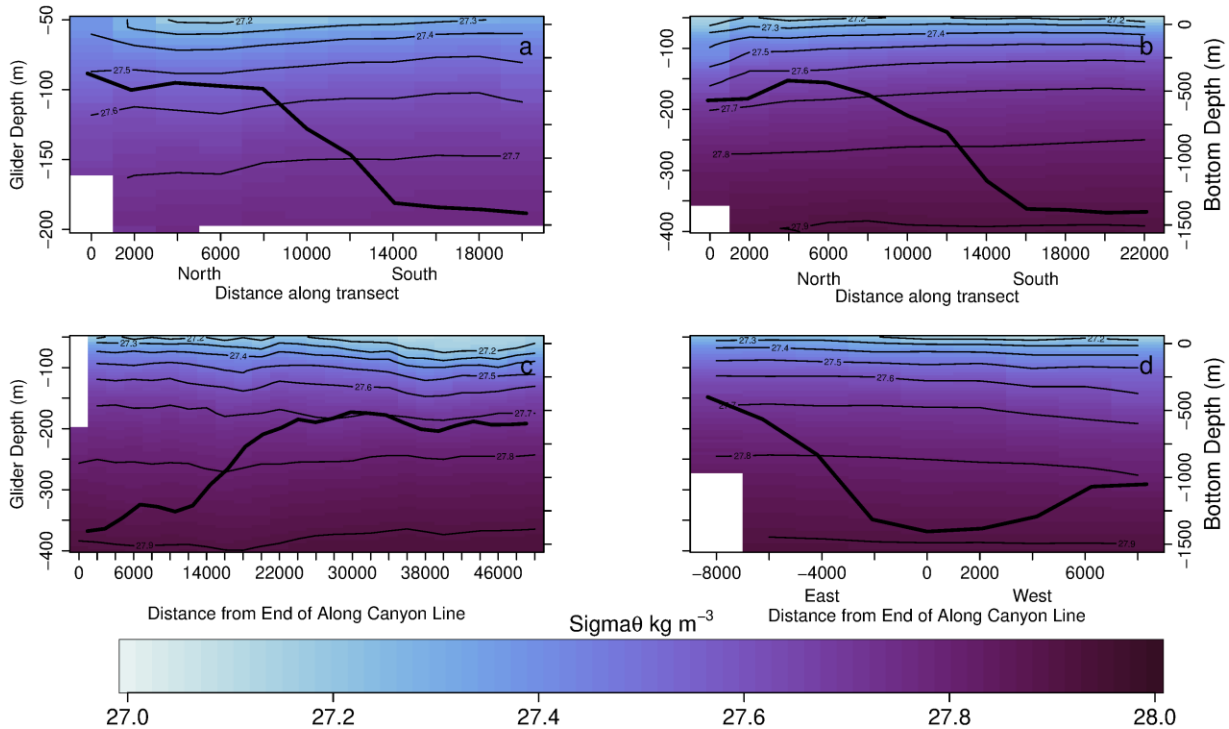

Figure 4. Average σθ cross sections from the along-canyon (a-b), shelf-canyon (c), and deep across-canyon (d) transects observed by gliders in 2015 (a) and 2020 (b-d). Observations were averaged in 2 km bins in the horizontal and 5m bins in the vertical. The black line denotes the average canyon depth experienced by the glider and corresponds to the right y axis in each panel. Note that each panel starts at 50m and that transects from 2015 (a) are only plotted to 200m while the remaining panels are plotted to 400m.

3.1.3 High-Frequency Radar Observations

The HFR system observes surface currents, which are dominated by winds in the austral summer. To examine the surface expression of the eddy over the canyon, we examined the HFR data sampled in low wind periods to limit the effect of winds on the observed currents. There was a total of 8 periods in 2015 and 16 periods in 2020 of low winds (< 5 m s^{-1}) over the canyon (Figure S5). These time periods ranged from 12 – 100 hours in length (Figure S5). Across both years, most of these periods were dominated by strong flow from the southeast moving toward the northwest.

Only two time periods, one in each deployment year, showed cyclonic rotation over the canyon (Figure 5; regions shaded with dark grey lines in Figure S5). Currents ranged from approximately 5 to 15 cm s^{-1} in this surface feature (Figure 5). In 2015, this period occurred in late January and was 22 hours in length (Figure 5a; S5a). In 2020, cyclonic rotation was observed in early January (Figure S5b). In 2020, the low-wind period where cyclonic rotation

was observed was the longest low wind period (100 hours) of those considered here (Figure 5b; S5b). These low-wind incidences co-occurred with time periods of low stratification (Figure S5).

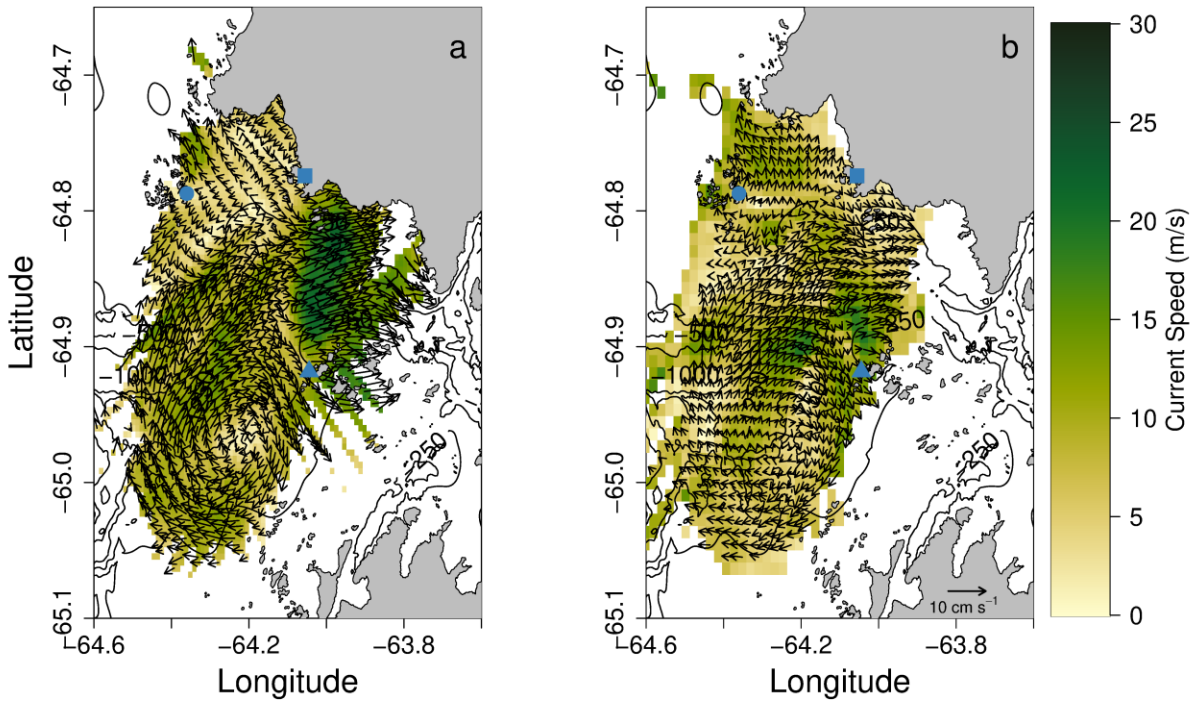

Figure 5. Mean High-Frequency Radar (HFR) fields over Palmer Deep Canyon during two low-wind periods in 2015 (a) and 2020 (b). HFR stations are marked with blue shapes and are the same as in Figure 1b.

3.2 Residence Times within the Subsurface Eddy

Simulated neutrally-buoyant particles were released into ROMS at the surface, 10, 20, 50, 120, 150, and 300 m throughout the austral summer. Residence times, for the most part, increased with depth. The median residence times increase from 4.1 ± 3.3 days at the surface to 166.6 ± 74 days at 150 m (Figure 6). Residence times decreased slightly between 150 and 300 m, from 166.6 ± 74 days to 132.3 ± 26.1 days, but these do not differ statistically (Figure 6). Shallow depths (10 and 20 m) were very similar (6.9 ± 4.2 and 7.4 ± 4.7 days, respectively) (Figure 6). Median residence times increase dramatically below 50 m, increasing from 18 ± 10.2 days at 50 m to 157.2 ± 86.8 days at 120 m (Figure 6). These residence times were much higher than residence times calculated on the continental shelf and the coast of Anvers Island (Figure 6). Residence times on the continental shelf ranged between 1.5 ± 0.7 and 2.3 ± 0.3 days over the same release depths while residence times on the coast of Anvers Island ranged between 2 ± 1.2

and 7.1 ± 3 days (Figure 6). Residence times in the top 20 m were more similar in PDC and the Anvers coast, but greatly differ starting at 50 m (Figure 6).

When compared statistically, the residence times over PDC varied significantly with depth ($p << 0.001$). In the top 50 m, residence times, for the most part, were not significantly different from each other ($0.107 < p < 1$). The only exception was that the surface and 50 m residence times differed significantly ($p < 0.001$). Similarly, residence times calculated between 120 and 150 m did not differ significantly ($p = 1$). However, when residence times were compared across shallow (≤ 50 m) and deep (≥ 50 m) particle releases, all comparisons differed significantly ($p << 0.001$). In comparison, only residence times on the continental shelf at 300 m were significantly different from other depths ($p << 0.001$). On the coast of Anvers Island, surface residence times were significantly lower than all other depths ($p << 0.001$). Residence times at 10 m were also significantly different from those at 300 m in this region ($p = 0.002$).

From December to February, shallow residence times (surface, 10, and 20 m) are relatively similar, increasing to a maximum of approximately 20 days in January (Figure S11). At 50 m, residence times are like shallower depths until late December, where the residence times increase to ~25-30 days until the end of the summer (Figure S11). At the depths with the greatest residence times (120 and 150 m), residence times increase from 10-20 days in early December to upwards of 300 days in mid-December, decreasing to 100-200 days at the end of the austral summer (Figure S11). The ROMS MLD shoals at approximately the same time (late December) that residence times at depth increase rapidly (Figure S12). At 300 m, residence times are relatively constant throughout the austral summer, ranging between ~100-175 days, with no

noticeable changes in response to changing stratification (Figure S11).

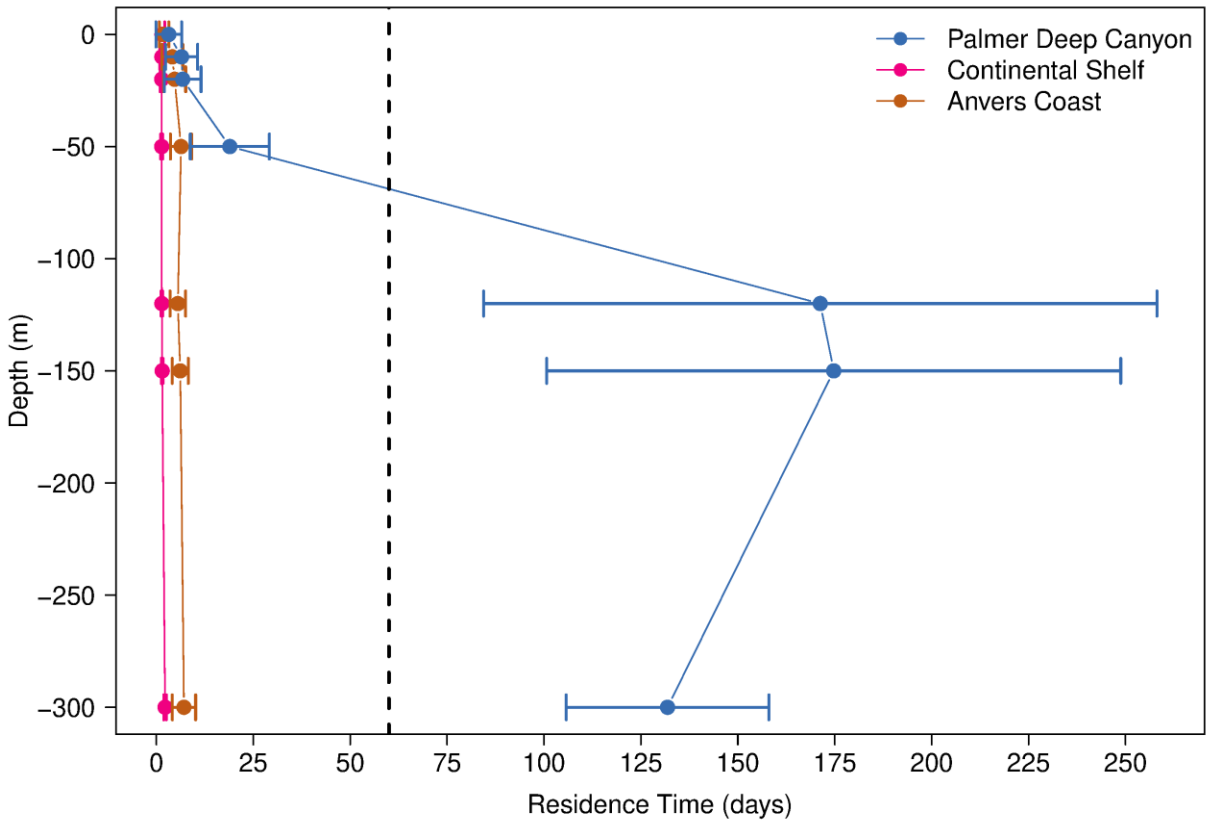

Figure 6. Median residence times (± 1 Standard Deviation) of summertime simulated particles released in ROMS at the surface, 10, 20, 50, 120, 150, and 300 m during the 2008-2009 season within the Palmer Deep Canyon (black), continental shelf (red), and Anvers Coast (blue) regions defined in Figure 1a. The vertical dashed line indicates a residence time of 60 days.

3.3 Subsurface Particle Layer

3.3.1 Glider Observations

The gliders observed a subsurface particle layer at ~75 - 120 m in both the 2015 and 2020 field campaigns (Figure 7). Optical backscatter was higher overall in 2015 in comparison to 2020 (Figure S13), possibly due to higher overall surface chlorophyll and particles in the area in 2015 (Figures S13-S15). Regardless, the overall patterns are similar between the along-canyon transects sampled in both field campaigns (Figure 7a-b). Increased optical backscatter (likely more particles) was observed over the deepest portions of the along-canyon transects (Figure 7a-b). On the shelf-canyon line (Figure 7c), increased concentrations of particles were observed as the glider moved over the sill separating the canyon from the continental shelf. In addition, there

was much lower optical backscatter on the continental shelf in comparison to areas within the canyon (Figure 7c), suggesting that the PDC is retaining these particles. On this transect, particle concentrations at depth were significantly higher in the PDC than on the shelf (Wilcoxon Rank Sum test, $p << 0.001$). Higher concentrations of particles were also observed on the deep across-canyon transect (Figure 7d). These increased concentrations were observed over the deepest portions of the canyon (Figure 7d), at similar depths to the particle layer observed in the along-canyon transect (Figure 7b).

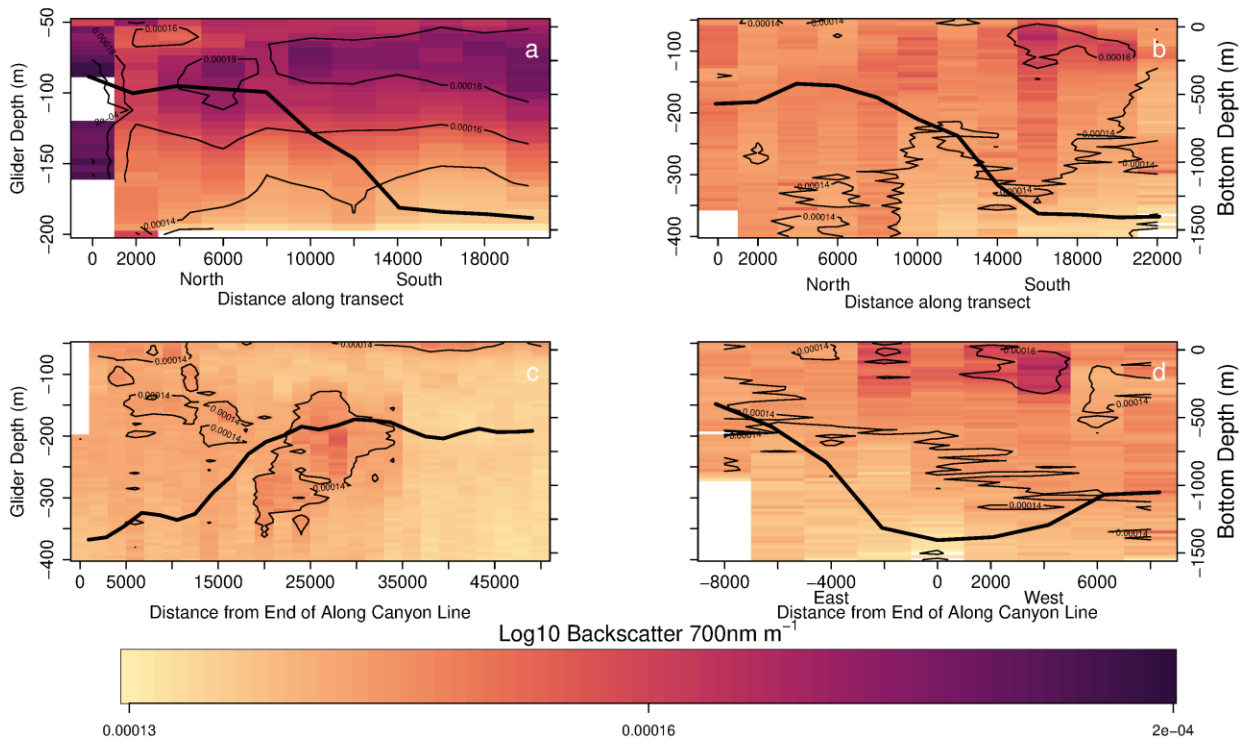

Figure 7. As in Figure 4, but with optical backscatter.

3.3.2 Identifying the Particles

On the first sampling event in early February (Figure 8a-c), live cell counts were highest in the surface and decreased with depth. At all three stations and depths, detritus cells outnumbered live cells (Figure 8a-c). At all three stations sampled, detritus cells increased below 75 m (Figure 8a-c). This increase was most prevalent at H5 (Figure 8a), over the canyon. On March 6 (Figure 8d-f), there were more live cells in the surface layer at all stations. This coincides with an increase in surface biomass (Figures S13-S14, S16). Particle counts still decreased with depth just as the live cell counts did in the previous sampling event (Figure 8a-c).

Overall, there were more detritus cells throughout the water column in the second sampling event in comparison to the first sampling event (Figure 8). At H5 and H3, the number of detrital cells increased dramatically at 75 m, rather than 100 m like in the previous sampling event and at H1 (Figure 8), suggesting that the particle layer had become shallower slightly over the canyon between sampling events.

Cells within the particle layer were predominately classified as detritus cells, with live cells making up a small percent of all cells within the layer across both sampling events (Figure 8). Images from the IFCB confirm that these cells appear to be detritus with many of them being amorphous (Figure 8, insets). Some particles look like small conglomerates (Figure 8b, detritus example from 200 m), while others look like clear material that may have been sloughed off in a molting event, or remains of a feeding event (Figure 8a, detritus example from 200 m). These particles had equivalent diameters on the order of 70 μm across both sampling events. These particle layers did not appear to be coincident with any pycnoclines or subsurface chlorophyll

maxima within the water column (Figures 8, S16-17).

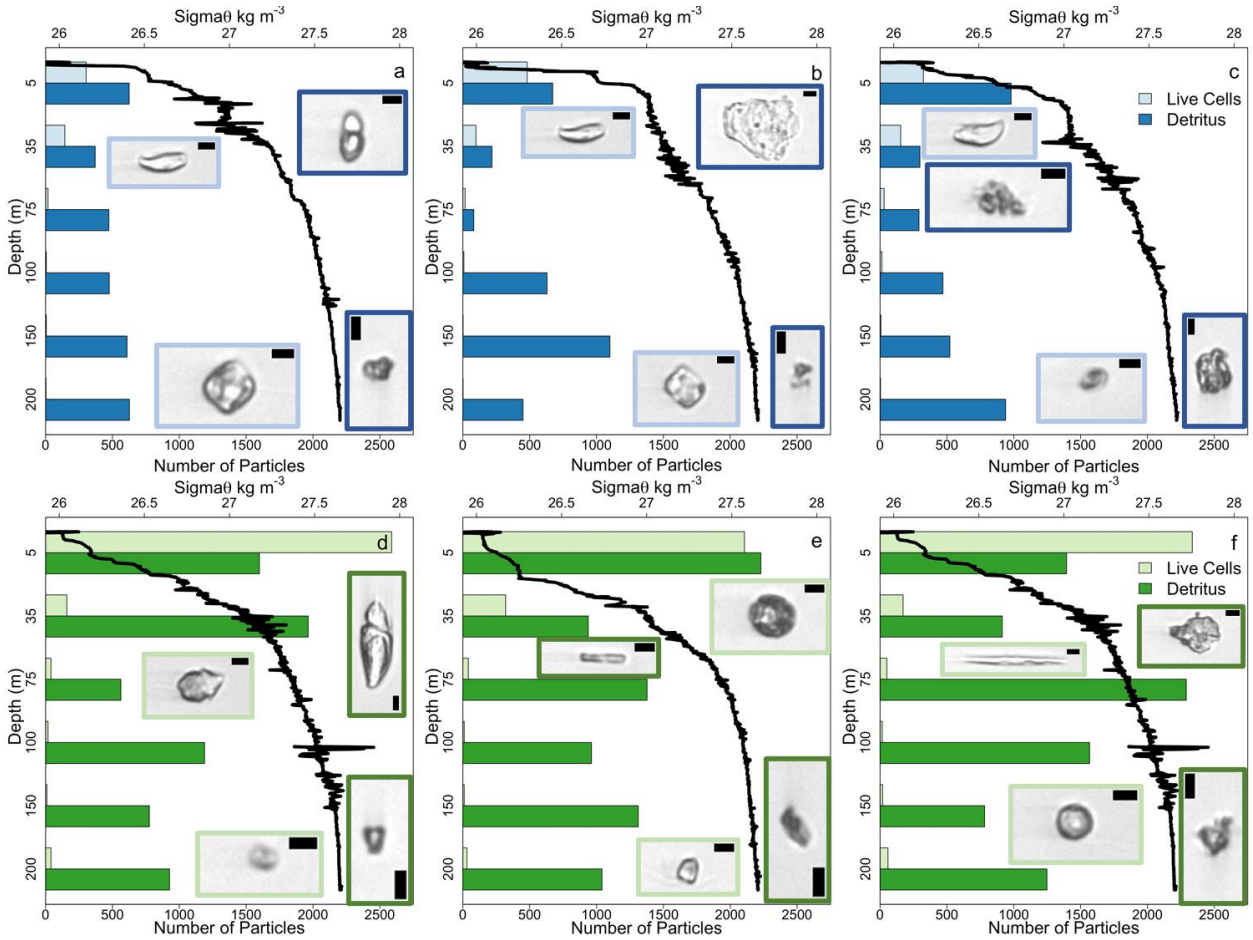

Figure 8. Number of particles (bars) for both live (light colors) and detritus (dark colors) particles counted by the IFCB at three stations: H1 (a, d), H3 (b, e), and H5 (c, f). The top row (a-c) illustrates data from the first IFCB sampling event on February 8, 2020 and the bottom row (d-f) represents data from the second sampling event on March 7, 2020. The black line on each panel represents σθ calculated from CTD casts during the sampling event. Photo insets depict examples of live (light border) and detritus (dark border) cells from 5 m (top) and 200 m (bottom) samples. Images represent particles of the approximate median equivalent diameter from each sample. A 5 μm scale bar is provided in each inset.

4 Discussion

4.1 The Subsurface Recirculating Eddy

Mean current velocities from the surface to 300 m illustrate cyclonic circulation over PDC during the austral summer (Figure 2). The cyclonic currents are on the order of 10 cm s^{-1} and rotate around a low-pressure system evident in the mean SSH anomaly from the model simulations (Figure 2). This rotation was not perfectly aligned with the canyon in the surface but is similar to the surface offset of the eddy in ROMS (Figures 2, 5), with the eddy displaced

slightly to the south of the canyon. Water moves along isobaths, driven by bathymetric steering and the low-pressure system observed in the SSH, as it moves into the canyon (Figure 2). These observations suggest that the flow is barotropic. This cyclonic circulation was also observed at the surface in long (> 12 hr) periods of low winds which coincided with periods of low stratification over the canyon (Figures 5, S5). We interpret this surface flow pattern at low winds and low stratification as circumstantial evidence that the subsurface, terrain following flow is, at least in part, barotropic.

Average cross sections from ROMS (Figure 3) and the glider deployments in both field campaigns (Figure 4) illustrate doming of isopycnals over PDC. These are most evident in the along-canyon and shelf-canyon lines (Figures 3a-b, 4a-c). On the along-canyon and shelf-canyon lines in both model simulations and glider observations, isopycnals become shallower as the canyon deepens. While the locations and depths of the isopycnals between ROMS and glider observations are not identical, the overall patterns of isopycnal doming are similar. This doming of isopycnals over the canyon suggests that there is a baroclinic component to the flow. How much of the flow is driven by baroclinic versus barotropic components should be investigated further.

The persistence of the eddy in the surface as predicted by the model was not observed in the HFR (Figure 2a, 5). The eddy was only present in the HFR field once in 2015 and once in 2020, while the model suggested it was a semi-persistent feature in the surface (Figure 2a). These differences may be due to factors that impact stratification and overall water column structure in the summer including variations in sea ice cover during the previous winter (Venables et al., 2013), amount and timing of ice melt (Venables et al., 2013; Vernet et al., 2008), wind mixing (Schofield et al., 2018), and other variables. The summer MLD over the canyon is lower in the model than the glider observations, especially in comparison to 2020 glider observations (Figure S12). This likely leads to the model surface layer being less isolated from the deep flow (i.e. the model circulation is more barotropic than observations) and may be why the observed surface circulation has less indication of the semi-permanent eddy than the model. ROMS simulations used for this study covered the 2008-09 austral summer, while our observations presented here are from 2015 and 2020. Nevertheless, we believe that these data support our hypothesis that a subsurface recirculating eddy is present within PDC during the austral summer.

4.2 The Retentive Properties of the Eddy

Simulated neutrally-buoyant particle experiments conducted with the numerical model illustrate that the residence time within PDC increases with depth (Figure 6). At depth (> 50m), residence times in PDC were much greater than residence times calculated on the nearby continental shelf and the coast of Anvers Island (Figure 6). Median residence times reached 166.6 ± 74 days at 150 m and decreased to 132.2 ± 26.1 days at 300 m (Figure 6). The residence times below 50 m are far longer than the peak biological season (60-75 days) in PDC, from mid-December to mid/late February. This suggests that particles could be retained within the system for the entire austral summer if they enter the system in the spring. These residence time calculations suggest that the eddy within PDC is highly retentive during the austral summer, especially as depth increases. The gliders deployed in 2020 also observed low oxygen saturations at depth within the canyon, indicating that organic matter is being either exported or retained in these regions, and that this water has not been in contact with the atmosphere for some time. (Figure S10; Levin, 2003; Sarmiento et al., 1988). This supports our hypothesis that the subsurface eddy is retentive.

Calculated residence times vary significantly between the surface and at depth within PDC (Figure 6). Particles between the surface and 50 m, for the most part, were not significantly different from each other. A similar pattern was observed in deep particles released between 120 and 300 m. When residence times were compared across these two groups, residence times differed significantly. This suggests that PDC is a two-layer system – a surface mixed layer with lower residence times and a deep layer with significantly higher residence times. A significant difference between the surface and 50 m residence times may suggest that 50 m is the approximate bottom of this surface layer in the model simulations. This layer may be shallower and may be correlated to the depth of the mixed layer. Previous glider-based observations within PDC also suggested that this two-layer water column structure is present within the region (Hudson et al., 2019). Spatial correlations of glider-measured temperature, salinity, and optical backscatter suggested that the surface of the waters in PDC have no correlation with the canyon below, while deep (~100 m) waters have strong correlation with the canyon below (Hudson et al., 2019). This similar dichotomy in the residence times in the surface versus at depth provides further evidence that the PDC is strongly shaping subsurface flow.

Residences times appear to vary seasonally, and these variations are amplified at depth. At the beginning of the simulation, residence times for particles released at 120 m were approximately 15 days (Figure S11). In mid-December, residence times spiked to approximately 200 days (Figure S11). There was another smaller spike at 50 m in late December, reaching a maximum of approximately 40 days (Figure S11). These spikes are coincident with the seasonal shoaling of the mixed layer and seasonal variations in model MLD (Figure S12). As the stratification increases at the beginning of the summer, less of the water column is impacted by surface forcing such as wind and more of the flow can be driven by the canyon bathymetry, thus trapping more particles in the canyon. At deeper depths (300m), residence times were relatively consistent over the course of the simulation with no changes corresponding with changes in stratification, suggesting that the increasing stratification increases residence times down to a specific depth, having no impact on residence times at depths deeper than this threshold, somewhere between 150 and 300 m.

While residence times in the surface are similar to previous studies based on *in-situ* observations (4.1 ± 3.3 days in this study vs 2.1 ± 0.9 days in Kohut et al. (2018)), residence times calculated at 150 m are over 100 days greater than previously calculated subsurface residence times for particles released at similar depths (166.6 ± 74 vs ~50 days) (Couto et al., 2017). Residence times closer to the surface (50 m) are similar to estimates made in previous ROMS studies (18 ± 10.2 days vs ~20 days) (Couto et al., 2017). These previous calculations were made with an older version of the circulation model with 4 km horizontal resolution, coarser and less accurate bathymetry for the region around PDC, and no tidal forcing. In addition, the particles simulated by Couto et al. (2017) were released over the canyon only in January over several model years, while particles in this study were released throughout the austral spring and summer of a single season. It is unclear whether the increased time period, model resolution, or the addition of tides are the cause of these differences. Preliminary comparisons of residence times in model runs with and without tides within the same season suggest that the addition of tides significantly increases residence times. It is possible that this increase is driven by tidal rectification taking place over PDC, where tides help constrain the flow over the canyon and thus increase residence times within the system (Loder, 1980), but this needs to be examined further.

4.3 The Subsurface Particle Layer

Over the deepest portions of the canyon in the along-canyon transect, the particle layer persisted between approximately 50 and 150 m, in both 2015 and 2020 (Figure 7a-b, 7d). There were almost no particles observed on the continental shelf outside of the canyon, and particle concentrations were significantly lower on the continental shelf outside PDC (Figure 7c). This provides further support for our hypothesis that the subsurface eddy generated by the canyon plays a role in retaining these particles for long periods of time.

Imaging the subsurface particle layer revealed that most of the particles in the water column and in the particle layer were detritus. This supports our hypothesis that particles would be marine snow, or detritus. Most suspended particles in the ocean are believed to be detritus, or aggregations of detritus, so this was expected (Alldredge & Silver, 1988). However, the median particle size, presented here as the equivalent diameter of the particles, was smaller than expected for marine snow, which is on the order of 500 μm (Alldredge & Silver, 1988). Instead of aggregates of marine snow, most particles in the particle layer were individual pieces ≤ 100 μm. In the particle layer at the most offshore stations (H5 and H3), median particle equivalent diameters were on the order of 70 μm.

Some cells within the particle layer did consist of small aggregations of even smaller individual cells but most appeared to be individual cells or cell fragments. Many particles looked like they had been sloughed off individuals in a molting or feeding event. They could have also been remnants of incomplete or ‘sloppy’ zooplankton feeding (Møller et al., 2003; Roy et al., 1989). It is also possible that these particles may have been remnants of larger, rapidly sinking particles from the surface layer (Bacon et al., 1985; Lal, 1980). While there were identifiable diatoms and other common phytoplankton cells in the surface, it was not possible to identify many of the particles in the subsurface layer. It is possible that these particles may have, at one point, been marine snow as originally hypothesized. These large aggregates could have been broken up *in-situ* by small zooplankton, during sampling, or by the IFCB. These particles are organic, and likely sourced from the surface layer. A lower concentration of particles in 2020 in comparison to 2015 and corresponding patterns in surface biomass seem to suggest the surface is a possible source for this particle layer. This would support the theory that suspended particle layers may be remnants of larger, rapidly sinking surface particles (Bacon et al., 1985; Lal, 1980).

4.4 Possible Implications for the Biological Hotspot

The particle layer retained within the canyon by this subsurface eddy could play a role in the biological hotspot. Sloppy feeding by zooplankton, which may help generate this layer, has been shown to act as a significant source of dissolved organic carbon to the microbial food web (Møller et al., 2003). In addition, subsurface organic particle layers worldwide have been associated with increased microbial activity (Alldredge & Silver, 1988; Garfield et al., 1983). Suspended subsurface particle layers may play a large role in sustaining mesopelagic heterotrophs (Baltar et al., 2009, 2010; Duret et al., 2019). Recent work has suggested that distinct microbial communities form on suspended versus sinking detritus particles in mesopelagic and mixed layers of the Scotia Sea, north of the WAP (Duret et al., 2019). These communities are uniquely adapted to utilize differing amounts of organic carbon and as a result play different roles in the biological carbon pump (Duret et al., 2019). The suspended particle layer in PDC may be like the layer observed in the Scotia Sea and may play a critical role in the local biological pump and remineralization of nutrients.

The subsurface particle layer may also act as an important food source for zooplankton within the PDC region. Isotope analysis around Hawaii has shown that micronekton become more reliant on suspended particles for food as their habitat depth increases (Gloeckler et al., 2018). The same study reported that several fish species were also found to be feeding primarily on suspended particles. Several detritivorous zooplankton species can be found at mesopelagic depths along the WAP (Conroy et al., 2020). These zooplankton species could potentially feed on the suspended subsurface particle layer, which ranged between 50-150 m, regardless of if they perform diel vertical migrations. Residence times at these depths ranged from 18 ± 10.2 and 167 ± 74 days (Figure 6), so this food source could persist through the austral summer at greater depths.

Antarctic krill have also been observed feeding on detritus (for example, Kawaguchi et al., 1986; Quetin & Ross, 1991; Schmidt et al., 2012, 2014; and others). Therefore, they could also potentially utilize the subsurface particle layer as a food source. However, it is unclear if and how often krill could utilize detritus as a food source during the austral summer. Most observations of krill feeding on detritus have been observed during the winter when food concentrations are low (Schmidt & Atkinson, 2016). If they feed on detritus in the austral

summer in similar conditions, it may be a key food source when chlorophyll concentrations are low, like in 2020 (Figures S13-14).

Since our observations are focused on the austral summer, it is unclear if the subsurface particle layer, and the eddy that may be responsible for retaining it over PDC, persists into winter. Daily mean currents at 100 m from ROMS suggest that the eddy is most persistent over PDC from mid-to-late December into early March (Supplementary Movie 1). However, the subsurface eddy may be present in a less persistent form during the winter months. Wintertime ROMS particle simulation observations of the subsurface particle layer are necessary to understand if this subsurface particle layer can act as a potentially critical food source for zooplankton in these food-limited months. If the subsurface eddy and the resulting suspended detritus particle layer are only present during the austral summer, it can still act as a critical food source for zooplankton, especially when phytoplankton are limited, during this time of increased biological activity in the region.

While beyond the scope of this analysis, it is also possible that the subsurface eddy retains zooplankton. Most zooplankton, including calanoid copepods, live at predominantly low Reynolds numbers (Koehl & Strickier, 1981; Price, 1988) and could, therefore, be trapped within this recirculating eddy, since they would not be able to swim against the prevailing currents. Zooplankton retention within eddies previously in the subarctic North Pacific (Mackas et al., 2005) and in the Irish Sea (Emsley et al., 2005). Zooplankton, including the Antarctic krill, are a critical food source for local predator species (W. Fraser & Hofmann, 2003; Pickett et al., 2018). Depending on their size, zooplankton may live at the low Reynold's numbers required to facilitate retention in the subsurface eddy. Many zooplankton perform diel vertical migrations, spending their days at depth, and feeding in the surface at night when visual predation risk is low (Hays, 2008). This behavior could significantly increase residence times of zooplankton within the system, especially with respect to the surface where residences times are predicted to be on the order of two to four days (Figure 6; Kohut et al., 2018). In comparison, residence times are ~150 days at depths as shallow as 120 m (Figure 6). These deep residence times are much longer than the peak biological activity in the region, which ranges from mid-December until mid-February (~60 days). Therefore, zooplankton that are advected into the system in the austral spring could be retained in the system through the austral summer. This vertical migration behavior may interact with the two-layer hydrography present within PDC as suggested by both

this study, previous glider observations (Hudson et al., 2019). Zooplankton may be retained at depth within the eddy during the day. At night, horizontal advection in the less retentive surface layer could transport zooplankton elsewhere. Previous krill distribution studies and HFR deployments suggested that flow over the canyon moves predominately towards shore (Kohut et al., 2018; Oliver et al., 2013). Zooplankton could possibly be advected into these nearshore regions during their time in the surface layer, where predator foraging activity is highest, therefore possibly contributing to the presence of this biological hotspot.

Acknowledgments, Samples, and Data

This project was funded through the National Science Foundation, Award Numbers 1327248 (2015) and 1744884 (2020) to UD, 1744884 to RU, and 1745011 to ODU. We are grateful to the Antarctic Support Contractor and their teams in Denver, CO, aboard the RVIB Laurence M. Gould, and at Palmer Station, without whom a project such as this would not be possible. We thank the students and field assistants from both projects for their valuable work on this project and the Palmer Antarctica Long-Term Ecological Research team for their involvement, suggestions, and collaboration. Computer simulations were run on the Wahab High Performance computing cluster at ODU.

Glider data used in this analysis can be accessed at the glider ERDDAP server (https://gliders.ioos.us/erddap/info/index.html). ROMS particle simulations; ROMS temperature, salinity, and density data; Imaging Flow Cytobot images and associated CTD data; and wind data will be archived at BCO-DMO (http://www.bco-dmo.org/) after the manuscript is accepted.

References

Alldredge, A. L., & Silver, M. W. (1988). Characteristics, dynamics and significance of marine snow. *Progress in Oceanography*, *20*(1), 41–82. https://doi.org/10.1016/0079-6611(88)90053-5

Bacon, M. P., Huh, C.-A., Fleer, A. P., & Deuser, W. G. (1985). Seasonality in the flux of natural radionuclides and plutonium in the deep Sargasso Sea. *Deep Sea Research Part A. Oceanographic Research Papers*, *32*(3), 273–286. https://doi.org/10.1016/0198-0149(85)90079-2

Baltar, F., Arístegui, J., Gasol, J. M., Sintes, E., & Herndl, G. J. (2009). Evidence of prokaryotic metabolism on suspended particulate organic matter in the dark waters of the subtropical North Atlantic. *Limnology and Oceanography*, *54*(1), 182–193. https://doi.org/10.4319/lo.2009.54.1.0182

Baltar, F., Arístegui, J., Sintes, E., Gasol, J. M., Reinthaler, T., & Herndl, G. J. (2010). Significance of non-sinking particulate organic carbon and dark CO2 fixation to heterotrophic carbon demand in the mesopelagic northeast Atlantic. *Geophysical Research Letters*, *37*(9). https://doi.org/10.1029/2010GL043105

Barrick, D. E., Lipa, B. J., & Crissman, R. D. (1985). Mapping surface currents with CODAR. *Sea Technology*, *26*(10), 43–48.

Budgell, W. P. (2005). Numerical simulation of ice-ocean variability in the Barents Sea region: Towards dynamical downscaling. *Ocean Dynamics*, *55*(3–4), 370–387. https://doi.org/10.1007/s10236-005-0008-3

Carvalho, F., Kohut, J., Oliver, M. J., Sherrell, R. M., & Schofield, O. (2016). Mixing and phytoplankton dynamics in a submarine canyon in the West Antarctic Peninsula: PHYTOPLANKTON DYNAMICS IN WAP CANYON. *Journal of Geophysical Research: Oceans*, *121*(7), 5069–5083. https://doi.org/10.1002/2016JC011650

Carvalho, F., Kohut, J., Oliver, M. J., & Schofield, O. (2017). Defining the ecologically relevant mixed-layer depth for Antarctica's coastal seas: MLD in Coastal Antarctica. *Geophysical Research Letters*, *44*(1), 338–345. https://doi.org/10.1002/2016GL071205

Carvalho, F., Fitzsimmons, J. N., Couto, N., Waite, N., Gorbunov, M., Kohut, J., et al. (2020). Testing the Canyon Hypothesis: Evaluating light and nutrient controls of phytoplankton growth in penguin foraging hotspots along the West Antarctic Peninsula. *Limnology and Oceanography*, *65*(3), 455–470. https://doi.org/10.1002/lno.11313

Conroy, J. A., Steinberg, D. K., Thibodeau, P. S., & Schofield, O. (2020). Zooplankton diel vertical migration during Antarctic summer. *Deep Sea Research Part I: Oceanographic Research Papers*, *162*, 103324. https://doi.org/10.1016/j.dsr.2020.103324

Couto, N., Kohut, J., Schofield, O., Dinniman, M., & Graham, J. (2017). Pathways and retention times in a biologically productive canyon system on the West Antarctic Peninsula. *OCEANS 2017 - Anchorage*, 1–8.

Dinniman, M. S., Klinck, J. M., & Smith, W. O. (2011). A model study of Circumpolar Deep Water on the West Antarctic Peninsula and Ross Sea continental shelves. *Deep Sea Research Part II: Topical Studies in Oceanography*, *58*(13–16), 1508–1523. https://doi.org/10.1016/j.dsr2.2010.11.013

Dinniman, M. S., Klinck, J. M., & Hofmann, E. E. (2012). Sensitivity of Circumpolar Deep Water Transport and Ice Shelf Basal Melt along the West Antarctic Peninsula to Changes in the Winds. *Journal of Climate*, *25*(14), 4799–4816. https://doi.org/10.1175/JCLI-D-11-00307.1

Duret, M. T., Lampitt, R. S., & Lam, P. (2019). Prokaryotic niche partitioning between suspended and sinking marine particles. *Environmental Microbiology Reports*, *11*(3), 386–400. https://doi.org/10.1111/1758-2229.12692

Emsley, S. M., Tarling, G. A., & Burrows, M. T. (2005). The effect of vertical migration strategy on retention and dispersion in the Irish Sea during spring–summer. *Fisheries Oceanography*, *14*(3), 161–174. https://doi.org/10.1111/j.1365-2419.2005.00327.x

Emslie, S., Fraser, W., Smith, R., & Walker, W. (1998). Abandoned penguin colonies and environmental change in the Palmer Station area, Anvers Island, Antarctic Peninsula. *Antarctic Science*, *10*, 257–268. https://doi.org/10.1017/S0954102098000352

Emslie, S. D., & Patterson, W. P. (2007). Abrupt recent shift in 13C and 15N values in Adelie penguin eggshell in Antarctica. *Proceedings of the National Academy of Sciences*, *104*(28), 11666–11669. https://doi.org/10.1073/pnas.0608477104

Fraser, W., & Hofmann, E. (2003). A predator's perspective on causal links between climate change, physical forcing and ecosystem response. *Marine Ecology Progress Series*, *265*, 1–15. https://doi.org/10.3354/meps265001

Fraser, W. R., & Trivelpiece, W. Z. (1996). Factors controlling the distribution of seabirds: Winter-summer heterogeneity in the distribution of adélie penguin populations. In E. E. Hofmann, R. M. Ross, & L. B.

Quetin (Eds.), *Antarctic Research Series* (Vol. 70, pp. 257–272). Washington, D. C.: American Geophysical Union. https://doi.org/10.1029/AR070p0257

Fretwell, P., Pritchard, H. D., Vaughan, D. G., Bamber, J. L., Barrand, N. E., Bell, R., et al. (2013). Bedmap2: improved ice bed, surface and thickness datasets for Antarctica. *The Cryosphere*, *7*(1), 375–393. https://doi.org/10.5194/tc-7-375-2013

Garfield, P. C., Packard, T. T., Friederich, G. E., & Codispoti, L. A. (1983). A subsurface particle maximum layer and enhanced microbial activity in the secondary nitrite maximum of the northeastern tropical Pacific Ocean. *Journal of Marine Research*, *41*(4), 747–768. https://doi.org/10.1357/002224083788520496

Gloeckler, K., Choy, C. A., Hannides, C. C. S., Close, H. G., Goetze, E., Popp, B. N., & Drazen, J. C. (2018). Stable isotope analysis of micronekton around Hawaii reveals suspended particles are an important nutritional source in the lower mesopelagic and upper bathypelagic zones. *Limnology and Oceanography*, *63*(3), 1168–1180. https://doi.org/10.1002/lno.10762

Graham, J. A., Dinniman, M. S., & Klinck, J. M. (2016). Impact of model resolution for on-shelf heat transport along the West Antarctic Peninsula. *Journal of Geophysical Research: Oceans*, *121*(10), 7880–7897. https://doi.org/10.1002/2016JC011875

Haidvogel, D. B., Arango, H., Budgell, W. P., Cornuelle, B. D., Curchitser, E., Di Lorenzo, E., et al. (2008). Ocean forecasting in terrain-following coordinates: Formulation and skill assessment of the Regional Ocean Modeling System. *Journal of Computational Physics*, *227*(7), 3595–3624. https://doi.org/10.1016/j.jcp.2007.06.016

Hays, G. C. (2008). A review of the adaptive significance and ecosystem consequences of zooplankton diel vertical migrations. *Hydrobiologica*, *503*, 163–170.

Holland, D. M., & Jenkins, A. (1999). Modeling Thermodynamic Ice–Ocean Interactions at the Base of an Ice Shelf. *JOURNAL OF PHYSICAL OCEANOGRAPHY*, *29*, 15.

Hudson, K., Oliver, M. J., Bernard, K., Cimino, M. A., Fraser, W., Kohut, J., et al. (2019). Reevaluating the Canyon Hypothesis in a Biological Hotspot in the Western Antarctic Peninsula. *Journal of Geophysical Research: Oceans*, *124*(8), 6345–6359. https://doi.org/10.1029/2019JC015195

Hunter, J. R., Craig, P. D., & Phillips, H. E. (1993). On the use of random walk models with spatially variable diffusivity. *Journal of Computational Physics*, *106*(2), 366–376. https://doi.org/10.1016/S0021-9991(83)71114-9

Kavanaugh, M., Abdala, F., Ducklow, H., Glover, D., Fraser, W., Martinson, D., et al. (2015). Effect of continental shelf canyons on phytoplankton biomass and community composition along the western Antarctic Peninsula. *Marine Ecology Progress Series*, *524*, 11–26. https://doi.org/10.3354/meps11189

Kawaguchi, K., Matsuda, O., Ishikawa, S., & Naito, Y. (1986). A light trap to collect krill and other micronektonic and planktonic animals under the Antarctic coastal fast ice. *Polar Biology*, *6*(1), 37–42. https://doi.org/10.1007/BF00446238

Kelley, D., & Richards, C. (2020). oce: Analysis of Oceanographic Data (Version R package version 1.2-0). Retrieved from https://CRAN.R-project.org/package=oce

Koehl, M. a. R., & Strickier, J. R. (1981). Copepod feeding currents: Food capture at low Reynolds number1. *Limnology and Oceanography*, *26*(6), 1062–1073. https://doi.org/10.4319/lo.1981.26.6.1062

Kohut, J. T., Winsor, P., Statscewich, H., Oliver, M. J., Fredj, E., Couto, N., et al. (2018). Variability in summer surface residence time within a West Antarctic Peninsula biological hotspot. *Philosophical Transactions of the Royal Society A: Mathematical, Physical and Engineering Sciences*, *376*(2122), 20170165. https://doi.org/10.1098/rsta.2017.0165

Lal, D. (1980). Comments on some aspects of particulate transport in the oceans. *Earth and Planetary Science Letters*, *49*(2), 520–527. https://doi.org/10.1016/0012-821X(80)90093-X

Levin, L. A. (2003). OXYGEN MINIMUM ZONE BENTHOS: ADAPTATION AND COMMUNITY RESPONSE TO HYPOXIA. *Oceanography and Marine Biology: An Annual Review*, *41*, 1–45.

Loder, J. (1980). Topographic Rectification of Tidal Currents on the Sides of Georges Bank. *J. Phys. Oceanogr.; (United States)*, *10:9*. https://doi.org/10.1175/1520-0485(1980)010<1399:TROTCO>2.0.CO;2

Mackas, D. L., Tsurumi, M., Galbraith, M. D., & Yelland, D. R. (2005). Zooplankton distribution and dynamics in a North Pacific Eddy of coastal origin: II. Mechanisms of eddy colonization by and retention of offshore species. *Deep Sea Research Part II: Topical Studies in Oceanography*, *52*(7), 1011–1035. https://doi.org/10.1016/j.dsr2.2005.02.008

Martinson, D. G., & McKee, D. C. (2012). Transport of warm Upper Circumpolar Deep Water onto the western Antarctic Peninsula continental shelf. *Ocean Science*, *8*(4), 433–442. https://doi.org/10.5194/os-8-433-2012

Moffat, C., Owens, B., & Beardsley, R. C. (2009). On the characteristics of Circumpolar Deep Water intrusions to the west Antarctic Peninsula Continental Shelf. *Journal of Geophysical Research*, *114*(C5). https://doi.org/10.1029/2008JC004955

Moline, M. A. (1998). *Temporal dynamics and regulation of coastal Antarctic phytoplankton communities: Spring/summer 1991-1994* (Doctoral dissertation). University of California Santa Barbara.

Møller, E., Thor, P., & Nielsen, T. (2003). Production of DOC by Calanus finmarchicus, C. glacialis and C. hyperboreus through sloppy feeding and leakage from fecal pellets. *Marine Ecology Progress Series*, *262*, 185–191. https://doi.org/10.3354/meps262185

Oliver, M. J., Irwin, A., Moline, M. A., Fraser, W., Patterson, D., Schofield, O., & Kohut, J. (2013). Adélie Penguin Foraging Location Predicted by Tidal Regime Switching. *PLoS ONE*, *8*(1), e55163. https://doi.org/10.1371/journal.pone.0055163

Oliver, M. J., Kohut, J. T., Bernard, K., Fraser, W., Winsor, P., Statscewich, H., et al. (2019). Central place foragers select ocean surface convergent features despite differing foraging strategies. *Scientific Reports*, *9*(1). https://doi.org/10.1038/s41598-018-35901-7

Olson, R. J., & Sosik, H. M. (2007). A submersible imaging-in-flow instrument to analyze nano-and microplankton: Imaging FlowCytobot. *Limnology and Oceanography: Methods*, *5*(6), 195–203. https://doi.org/10.4319/lom.2007.5.195

Padman, L., Fricker, H. A., Coleman, R., Howard, S., & Erofeeva, L. (2002). A new tide model for the Antarctic ice shelves and seas. *Annals of Glaciology*, *34*, 247–254. https://doi.org/10.3189/172756402781817752

Pickett, E. P., Fraser, W. R., Patterson-Fraser, D. L., Cimino, M. A., Torres, L. G., & Friedlaender, A. S. (2018). Spatial niche partitioning may promote coexistence of *Pygoscelis* penguins as climate-induced sympatry occurs. *Ecology and Evolution*, *8*(19), 9764–9778. https://doi.org/10.1002/ece3.4445

Piñones, A., Hofmann, E. E., Dinniman, M. S., & Klinck, J. M. (2011). Lagrangian simulation of transport pathways and residence times along the western Antarctic Peninsula. *Deep Sea Research Part II: Topical Studies in Oceanography*, *58*(13), 1524–1539. https://doi.org/10.1016/j.dsr2.2010.07.001

Powers, J. G., Manning, K. W., Bromwich, D. H., Cassano, J. J., & Cayette, A. M. (2012). A DECADE OF ANTARCTIC SCIENCE SUPPORT THROUGH AMPS. *Bulletin of the American Meteorological Society*, *93*(11), 1699–1712.

Prézelin, Barbara B., Hofmann, E. E., Mengelt, C., & Klinck, J. M. (2000). The linkage between Upper Circumpolar Deep Water (UCDW) and phytoplankton assemblages on the west Antarctic Peninsula continental shelf. *Journal of Marine Research*, *58*(2), 165–202. https://doi.org/10.1357/002224000321511133

Prézelin, B.B., Hofmann, E. E., Moline, M., & Klinck, J. M. (2004). Physical forcing of phytoplankton community structure and primary production in continental shelf waters of the Western Antarctic Peninsula. *Journal of Marine Research*, *62*(3), 419–460. https://doi.org/10.1357/0022240041446173

Price, H. J. (1988). Feeding Mechanisms in Marine and Freshwater Zooplankton. *Bulletin of Marine Science*, *43*(3), 17.

Quetin, L. B., & Ross, R. M. (1991). Behavioral and Physiological Characteristics of the Antarctic Krill, *Euphausia superba*. *American Zoologist*, *31*(1), 49–63. https://doi.org/10.1093/icb/31.1.49

R Core Team. (2020). *R: A language and environment for statistical computing*. Vienna, Austria: R Foundation for Statistical Computing. Retrieved from www.R-project.org

Roy, S., Harris, R. P., & Poulet, S. A. (1989). Inefficient feeding by Calanus helgolandicus and Temora longicornis on Coscinodiscus wailesii: quantitative estimation using chlorophyll-type pigments and effects on dissolved free amino acids. *Marine Ecology Progress Series*, *52*(2), 145–153.

Ryan, W. B. F., Carbotte, S. M., Coplan, J. O., O'Hara, S., Melkonian, A., Arko, R., et al. (2009). Global Multi-Resolution Topography synthesis: GLOBAL MULTI-RESOLUTION TOPOGRAPHY SYNTHESIS. *Geochemistry, Geophysics, Geosystems*, *10*(3), n/a-n/a. https://doi.org/10.1029/2008GC002332

Sarmiento, J. L., Herbert, T. D., & Toggweiler, J. R. (1988). Causes of anoxia in the world ocean. *Global Biogeochemical Cycles*, *2*(2), 115–128. https://doi.org/10.1029/GB002i002p00115

Schmidt, K., & Atkinson, A. (2016). Feeding and Food Processing in Antarctic Krill (Euphausia superba Dana). In V. Siegel (Ed.), *Biology and Ecology of Antarctic Krill* (pp. 175–224). Cham: Springer International Publishing. https://doi.org/10.1007/978-3-319-29279-3_5

Schmidt, K., Atkinson, A., Venables, H. J., & Pond, D. W. (2012). Early spawning of Antarctic krill in the Scotia Sea is fuelled by "superfluous" feeding on non-ice associated phytoplankton blooms. *Deep Sea Research Part II: Topical Studies in Oceanography*, *59–60*, 159–172. https://doi.org/10.1016/j.dsr2.2011.05.002

Schmidt, K., Atkinson, A., Pond, D. W., & Ireland, L. C. (2014). Feeding and overwintering of Antarctic krill across its major habitats: The role of sea ice cover, water depth, and phytoplankton abundance. *Limnology and Oceanography*, *59*(1), 17–36. https://doi.org/10.4319/lo.2014.59.1.0017

Schofield, O., Ducklow, H., Bernard, K., Doney, S., Patterson-Fraser, D., Gorman, K., et al. (2013). Penguin Biogeography Along the West Antarctic Peninsula: Testing the Canyon Hypothesis with Palmer LTER Observations. *Oceanography*, *26*(3), 204–206. https://doi.org/10.5670/oceanog.2013.63

Schofield, O., Brown, M., Kohut, J., Nardelli, S., Saba, G., Waite, N., & Ducklow, H. (2018). Changes in the upper ocean mixed layer and phytoplankton productivity along the West Antarctic Peninsula. *Philosophical Transactions of the Royal Society A: Mathematical, Physical and Engineering Sciences*, *376*(2122), 20170173. https://doi.org/10.1098/rsta.2017.0173

Smith, R. C., Baker, K. S., Fraser, W. R., Hofmann, E. E., Karl, D. M., Klinck, J. M., et al. (1995). The Palmer LTER: A Long-Term Ecological Research Program at Palmer Station, Antarctica. *Oceanography*, *8*(3), 77–86.

Venables, H. J., Clarke, A., & Meredith, M. P. (2013). Wintertime controls on summer stratification and productivity at the western Antarctic Peninsula. *Limnology and Oceanography*, *58*(3), 1035–1047. https://doi.org/10.4319/lo.2013.58.3.1035

Vernet, M., Martinson, D., Iannuzzi, R., Stammerjohn, S., Kozlowski, W., Sines, K., et al. (2008). Primary production within the sea-ice zone west of the Antarctic Peninsula: I—Sea ice, summer mixed layer, and irradiance. *Deep Sea Research Part II: Topical Studies in Oceanography*, *55*(18–19), 2068–2085. https://doi.org/10.1016/j.dsr2.2008.05.021

Visser, A. (1997). Using random walk models to simulate the vertical distribution of particles in a turbulent water column. *Marine Ecology Progress Series*, *158*, 275–281. https://doi.org/10.3354/meps158275